Electronic Supplementary Material (ESI) for Green Chemistry.
This journal is © The Royal Society of Chemistry 2023

Supporting Information for:

Functionally Enhanced Basic Amino Acid-Based Binary Organocatalysts Based on Physical Doping for Efficient Coupling of CO_2 with Epoxides

Fan Wang,[a, b] Congxia Xie,[a] Hongbing Song,[b] and Xin Jin*[b]

[a] *College of Chemistry and Molecular Engineering, Qingdao University of Science and Technology, 53 Zhengzhou Road, Qingdao 266042, China*

[b] *College of Chemical Engineering, Qingdao University of Science and Technology, 53 Zhengzhou Road, Qingdao 266042, China*

Corresponding Author:

*** *E*-mail: Xin Jin, jinx1971@163.com**

List of the contents

1 Experimental Section

1.1 Materials

1.2 Characterization methods

1.3 Synthesis and characterization of [TMG-H][Br]

1.4 Synthesis and characterization of [TMG-H][I]

1.5 Synthesis and characterization of [MTBD-H][Br]

1.6 Synthesis and characterization of [$Me(EO)_4$TMG-H][Br]

1.7 Synthesis and characterization of [$Me(EO)_{16}$TMG-H][Br]

1.8 Synthesis and characterization of [$Me(EO)_{16}$TMG-H][I]

1.9 Preparation of binary catalyst *L*-Arg/[TMG-H][Br]

1.10 Preparation of binary catalyst *L*-Arg/[TMG-H][I]

1.11 Preparation of binary catalyst *L*-Arg/[MTBD-H][Br]

1.12 Preparation of binary catalyst *L*-Arg/[$Me(EO)_4$TMG-H][Br]

1.13 Preparation of binary catalyst *L*-Arg/[$Me(EO)_{16}$TMG-H][Br]

1.14 Preparation of binary catalyst *L*-Arg/[$Me(EO)_{16}$TMG-H][I]

1.15 Preparation of binary catalyst *L*-His/[$Me(EO)_{16}$TMG-H][Br]

1.16 Preparation of binary catalyst *L*-Lys/[$Me(EO)_{16}$TMG-H][Br]

1.17 Typical procedure for coupling of CO_2 with epoxides catalyzed by binary BAAs/PGILs catalysts

1.18 Typical procedure for recycling binary BAAs/PGILs catalysts in coupling reaction of CO_2 with epoxides

2 C1s XPS spectra of [$Me(EO)_{16}$TMG-H][Br], [TMG-H][Br], *L*-Arg/[$Me(EO)_{16}$TMG-H][Br] and *L*-Arg/[TMG-H][Br] (Figure S1)

3 Structure characterizations of binary *L*-Arg/[$Me(EO)_{16}$TMG-H][Br] catalyst (Figure S2)

4 2D ROESY NMR spectrum of *L*-Arg + [$Me(EO)_{16}$TMG-H][Br] (Figure S3)

5 The reaction kinetic study expressed as curves for TON *versus* time for the CO_2/SO coupling catalyzed by the binary catalysts *L*-Arg/[$Me(EO)_{16}$TMG-H][I] and *L*-Arg/[TMG-H][I] (Figure S4)

6 The catalyst stability tested by recycle experiments and corresponding kinetic curves of TON *versus* time in the CO_2/SO coupling reaction using the binary *L*-Arg/[TMG-H][I] catalyst (Figure S5)

7 The catalyst stability characterized by ^{1}H NMR and FT-IR spectra of *L*-Arg/[$Me(EO)_{16}$TMG-H][I] catalyst in cycloaddition reaction of CO_2 and SO (Figure S6)

8 Partial ^{1}H NMR spectra of [*L*-Arg-H][Br]/PO/PC and [$Me(EO)_{16}$TMG-H][Br]/PO/PC for recognizing the activation of PO by H-bonding (Figure S7)

9 Effect of reaction temperature on reaction kinetics in the CO_2/SO coupling reaction: evolution of ln[SO] with time at four different temperatures for *L*-Arg/[$Me(EO)_{16}$TMG-H][Br], *L*-Arg/[TMG-H][Br] and [$Me(EO)_{16}$TMG-H][Br] catalysts (Figure S8)

10 NMR Spectra

10.1 ^{1}H NMR spectrum of [TMG-H][Br] (Figure S9)

10.2 ^{1}H NMR spectrum of [TMG-H][I] (Figure S10)

10.3 ^{1}H NMR spectrum of [MTBD-H][Br] (Figure S11)

10.4 ^{1}H NMR spectrum of [Me(EO)$_4$TMG-H][Br] (Figure S12)

10.5 ^{13}C NMR spectrum of [Me(EO)$_4$TMG-H][Br] (Figure S13)

10.6 ^{1}H NMR spectrum of [Me(EO)$_{16}$TMG-H][Br] (Figure S14)

10.7 ^{13}C NMR spectrum of [Me(EO)$_{16}$TMG-H][Br] (Figure S15)

10.8 ^{1}H NMR spectrum of [Me(EO)$_{16}$TMG-H][I] (Figure S16)

10.9 ^{13}C NMR spectrum of [Me(EO)$_{16}$TMG-H][I] (Figure S17)

10.10 ^{1}H NMR spectrum of **2a** (Figure S18)

10.11 ^{1}H NMR spectrum of **2b** (Figure S19)

10.12 ^{1}H NMR spectrum of **2c** (Figure S20)

10.13 ^{1}H NMR spectrum of **2d** (Figure S21)

10.14 ^{1}H NMR spectrum of **2e** (Figure S22)

10.15 ^{1}H NMR spectrum of **2f** (Figure S23)

10.16 ^{1}H NMR spectrum of **2g** (Figure S24)

10.17 ^{1}H NMR spectrum of **2h** (Figure S25)

11 MS Spectra

11.1 Mass spectrum (ESI positive) of [Me(EO)$_4$TMG-H][Br] (Figure S26)

11.2 Mass spectrum (ESI negative) of [Me(EO)$_4$TMG-H][Br] (Figure S27)

11.3 Mass spectrum (ESI positive) of [Me(EO)$_{16}$TMG-H][Br] (Figure S28)

11.4 Mass spectrum (ESI negative) of [Me(EO)$_{16}$TMG-H][Br] (Figure S29)

11.5 Mass spectrum (ESI positive) of [Me(EO)$_{16}$TMG-H][I] (Figure S30)

11.6 Mass spectrum (ESI negative) of [Me(EO)$_{16}$TMG-H][I] (Figure S31)

References

1 Experimental Section

1.1 Materials

Unless specified, all the chemicals were purchased from commercial sources and used without further purification. All reagents and organic solvents were rigorously dehydrated by the standard purification methods before use.[1] The ILs [Me(EO)$_n$TMG-H][OMs] (n = 4, 16) were synthesized according to the method described in the literature.[2] Carbon dioxide with the purity of 99.999% was supplied by Qingdao Heli Gases Co. Ltd. The CO_2/epoxides coupling reactions were carried out in a 60 mL stainless-steel (316 L) autoclave.

1.2 Characterization

The products of CO_2/epoxides coupling were analyzed based on the internal standard method on GC equipped with an OV-101 capillary column (50 m × 0.25 μm) and FID. NMR (^{1}H, ^{13}C, 2D ROESY) spectra were recorded on the Bruker Avance 500 or Bruker Avance III 600 spectrometers. FT-IR analysis was conducted using the coating method (KBr window plate) on a Bruker VERTEX 70 FT-IR spectrometer with a resolution of 4 cm^{-1} in the range 400–4000 cm^{-1}. *In situ* diffuse reflectance infrared Fourier transform spectroscopy (DRIFTS) experiments were performed using a Thermo Fisher Scientific Nicolet iS50 FT-IR fitted with a fiber optical probe. Mass spectra (MS) were obtained by the electrospray technique using a Thermo Fisher Scientific LTQ Orbitrap XL mass spectrometry. TGA was performed from room temperature to 800 °C under N_2 flow using a Perkin-Elmer STA 8000 Simultaneous Thermal Analyzer with a ramp rate of 10 °C min^{-1}. X-ray photoelectron spectroscopy (XPS) analysis was obtained on a Thermo Fisher Scientific ESCALAB 250Xi spectrometer with Al *K*α (*hν* = 1486.6 eV) source using the Au 4F7/2 peak (binding energy: 84.0 eV) as the calibration of energy scale and the C1s peak at 284.8 eV as the internal standard. X-ray diffraction (XRD) patterns were observed using a Bruker D8 X-ray diffractometer with Cu-*K*α radiation (40 kV, 40 mA), and the corresponding data were collected at a scanning speed of 10° min^{-1} in the range of 5°-90° (2θ) with a step size of 0.020°. The high magnification photographs were taken by a Phenix PH100 optical microscope at ambient temperature.

1.3 Synthesis and characterization of [TMG-H][Br]

To TMG (2.5 g, 21.7 mmol) in 5 mL deionized water was added 48% of HBr aqueous solution (3.3 g, 19.6 mmol), and the reaction mixture was stirred at room temperature for 1 h. The water was removed by evaporation, and then the resulting white powder was washed with ethyl acetate (5 mL × 4), filtered and dried in vacuo to give the target product (3.7 g, 97 % yield). Characterization: ^{1}H NMR (500 MHz, D_2O): δ = 3.010 (s, 12H, $N(CH_3)_2$ × 2)

1.4 Synthesis and characterization of [TMG-H][I]

To TMG (3.7 g, 32.1 mmol) in 5 mL deionized water was added 57% of HI aqueous solution (6.0 g, 26.7mmol), and the reaction mixture was stirred at room temperature for 1 h. The water was removed by evaporation, and then the resulting yellow powder was washed with ethyl acetate (5 mL × 4), filtered and dried in vacuo to give the target product (6.2 g, 95 % yield). Characterization: ^{1}H NMR (500 MHz, D_2O): δ = 3.011 (s, 12H, $N(CH_3)_2$ × 2)

1.5 Synthesis and characterization of [MTBD-H][Br]

To MTBD (0.43 g, 2.8 mmol) in 5 mL deionized water was added 48% of HBr aqueous solution (0.44 g, 2.6 mmol), and the reaction mixture was stirred at room temperature for 1 h. The water was removed by evaporation, and then the resulting white powder was washed with ethyl acetate (2 mL × 4), filtered and dried in vacuo to give the target product (0.58 g, 95 % yield). Characterization: ^{1}H NMR (500 MHz, D_2O): δ = 3.329-3.261 (m, 8H, CH_2), 2.902 (s, 3H, CH_3), 1.976 (qui, 2H, CH_2), 1.925 (qui, 2H, CH_2).

1.6 Synthesis and characterization of [Me(EO)$_4$TMG-H][Br]

To [Me(EO)$_4$TMG-H][OMs](1.0 g, 2.5 mmol) in 20 mL acetonitrile was added NaBr (0.5 g, 4.9 mmol), and the reaction mixture was stirred at room temperature for 72 h. The resulting precipitate was removed by filtration, and then the acetonitrile in the filtrate was evaporated under reduced pressure to give the target product as a yellow viscous liquid (0.9 g, 93% yield). Characterization: ^{1}H NMR (500 MHz, D_2O): δ = 3.762-3.653 (m, 16H, OCH_2CH_2), 3.431 (t, 2H, OCH_2CH_2), 3.414 (s, 3H, OCH_3),

3.004 (s, 12H, $N(CH_3)_2$ × 2); ^{13}C NMR (126 MHz, $CDCl_3$): δ =162.447, 71.753, 70.377-70.164, 69.510, 58.807, 44.711, 40.492, 39.999; HRMS (ESI positive): m/z = 306.2389, calcd for $C_{14}H_{32}O_4N_3$ ($[CH_3(OCH_2CH_2)_4TMG\text{-}H]^+$): 306.2387; MS (ESI negative): m/z = 78.92, 80.92, calcd for Br^-: 78.92, 80.92.

1.7 Synthesis and characterization of $[Me(EO)_{16}TMG\text{-}H][Br]$

To $[Me(EO)_{16}TMG\text{-}H][OMs]$(5.0 g, 5.4 mmol) in 30 mL acetonitrile was added NaBr (1.7 g, 16.5 mmol), and the reaction mixture was stirred at room temperature for 72 h. The resulting precipitate was removed by filtration, and then the acetonitrile in the filtrate was evaporated under reduced pressure to give the target product as a yellow viscous liquid (4.6 g, 93% yield). Characterization: ^1H NMR (500 MHz, D_2O): δ = 3.736-3.649 (m, 66H), 3.430 (t, 2H), 3.415 (s, 3H), 3.003 (s, 12H); ^{13}C NMR (126 MHz, $CDCl_3$): δ = 162.433, 71.754, 70.354-70.151, 69.484, 58.806, 44.681, 40.468, 39.957; MS (ESI positive): m/z = 834.55, calcd for $C_{38}H_{80}O_{16}N_3$ ($[CH_3(OCH_2CH_2)_{16}TMG\text{-}H]^+$): 834.55; MS (ESI negative): m/z = 78.92, 80.92, calcd for Br^-: 78.92, 80.92.

1.8 Synthesis and characterization of $[Me(EO)_{16}TMG\text{-}H][I]$

To $[Me(EO)_{16}TMG\text{-}H][OMs]$(5.7 g, 6.1 mmol) in 40 mL acetonitrile was added NaI (2.8 g, 18.7 mmol), and the reaction mixture was stirred at room temperature for 96 h. The resulting precipitate was removed by filtration, and then the acetonitrile in the filtrate was evaporated under reduced pressure to give the target product as a yellow viscous liquid (5.7 g, 96% yield). Characterization: ^1H NMR (500 MHz, D_2O): δ = 3.717-3.630 (m, 68H), 3.405 (t, 2H), 3.392 (s, 3H), 2.979 (s, 12H); ^{13}C NMR (151 MHz, $CDCl_3$): δ = 162.508, 71.824, 70.419-70.227, 69.559, 58.903, 44.750, 40.599, 39.992; HRMS (ESI positive): m/z = 834.5546, calcd for $C_{38}H_{80}O_{16}N_3$ ($[CH_3(OCH_2CH_2)_{16}TMG\text{-}H]^+$): 834.5533; HRMS (ESI negative): m/z = 126.9050, calcd for I^-: 126.9050.

1.9 Preparation of binary catalyst *L*-Arg/[TMG-H][Br]

[TMG-H][Br] (0.74 g, 3.8 mmol) and *L*-Arg (0.66 g, 3.8 mmol) were mixed in H_2O (4 mL), and the mixture was stirred at room temperature for 5 h. The water was removed by evaporation, and then the resulting white powder was dried in vacuo to give the binary catalyst (1.4 g).

1.10 Preparation of binary catalyst *L*-Arg/[TMG-H][I]

[TMG-H][I] (1.56 g, 6.4 mmol) and *L*-Arg (1.12 g, 6.4 mmol) were mixed in H_2O (5 mL), and the mixture was stirred at room temperature for 5 h. The water was removed by evaporation, and then the resulting yellow powder was dried in vacuo to give the binary catalyst (2.68 g).

1.11 Preparation of binary catalyst *L*-Arg/[MTBD-H][Br]

[MTBD-H][Br] (0.43 g, 1.8 mmol) and *L*-Arg (0.32 g, 1.8 mmol) were mixed in H_2O (3 mL), and the mixture was stirred at room temperature for 5 h. The water was removed by evaporation, and then the resulting white powder was dried in vacuo to give the binary catalyst (0.75 g).

1.12 Preparation of binary catalyst *L*-Arg/$[Me(EO)_4TMG\text{-}H][Br]$

$[Me(EO)_4TMG\text{-}H][Br]$ (0.80 g, 2.1 mmol) and *L*-Arg (0.36 g, 2.1 mmol) were mixed in H_2O (4 mL), and the mixture was stirred at room temperature for 5 h. The water was removed by evaporation, and then the resulting cloudy viscous liquid was dried in vacuo to give the binary catalyst (1.16 g).

1.13 Preparation of binary catalyst *L*-Arg/$[Me(EO)_{16}TMG\text{-}H][Br]$

$[Me(EO)_{16}TMG\text{-}H][Br]$ (1.88 g, 2.1 mmol) and *L*-Arg (0.36 g, 2.1 mmol) were mixed in H_2O (5 mL), and the mixture was stirred at room temperature for 5 h. The water was removed by evaporation, and then the resulting cloudy viscous liquid was dried in vacuo to give the binary catalyst (2.24 g).

1.14 Preparation of binary catalyst *L*-Arg/$[Me(EO)_{16}TMG\text{-}H][I]$

$[Me(EO)_{16}TMG\text{-}H][I]$ (0.19 g, 0.2 mmol) and *L*-Arg (35.0 mg, 0.2 mmol) were mixed in H_2O (2 mL), and the mixture was stirred at room temperature for 5 h. The water was removed by evaporation, and then the resulting cloudy viscous liquid was dried in vacuo to give the binary catalyst (225 mg).

1.15 Preparation of binary catalyst *L*-His/$[Me(EO)_{16}TMG\text{-}H][Br]$

[Me(EO)$_{16}$TMG-H][Br] (1.00 g, 1.1 mmol) and *L*-His (0.17 g, 1.1 mmol) were mixed in H_2O (4 mL), and the mixture was stirred at room temperature for 5 h. The water was removed by evaporation, and then the resulting cloudy viscous liquid was dried in vacuo to give the binary catalyst (1.17 g).

1.16 Preparation of binary catalyst *L*-Lys/[Me(EO)$_{16}$TMG-H][Br]

[Me(EO)$_{16}$TMG-H][Br] (1.20 g, 1.3 mmol) and *L*-Lys (0.19 g, 1.3 mmol) were mixed in H_2O (4 mL), and the mixture was stirred at room temperature for 5 h. The water was removed by evaporation, and then the resulting cloudy viscous liquid was dried in vacuo to give the binary catalyst (1.39 g).

1.17 Typical procedure for coupling of CO_2 with epoxides catalyzed by binary BAAs/PGILs catalysts

Under an Argon atmosphere, epoxides (10.5 mmol) and binary catalyst *L*-Arg/[Me(EO)$_{16}$TMG-H][I] (0.0525 mmol/0.0525 mmol) were charged in a 60 mL stainless-steel autoclave equipped with a magnetic stirrer. The reaction mixture was heated to 110 °C, and then 1.5 MPa of CO_2 was introduced to autoclave. The reaction was carried out at 110 °C for desired time, and the autoclave was cooled to room temperature in ice water. After CO_2 was slowly released, methyl *tert*-butyl ether was added to extract the resulting products. The upper organic phase was separated, and the solvent and unconverted epoxides were removed under reduced pressure. Isolated products were identified by the ^{1}H NMR spectroscopy. Except for the PC yield calculated based on isolation, the yields of all other cyclic carbonates were determined by GC.

characterization of cyclic carbonates:

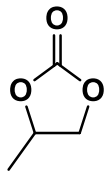

2a

4-methyl-1,3-dioxolan-2-one (2a): 75% isolated yield; ^{1}H NMR (500 MHz, $CDCl_3$): δ = 4.847 (m, 1H), 4.544 (t, *J* = 8.0 Hz, 1H), 4.014 (t, *J* = 8.0 Hz, 1H), 1.477 (d, *J* = 6.5 Hz, 3H).

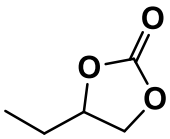

2b

4-ethyl-1,3-dioxolan-2-one (2b): 88% yield; ^{1}H NMR (500 MHz, $CDCl_3$): δ = 4.656 (m, 1H), 4.517 (t, *J* = 8.0 Hz, 1H), 4.074 (t, *J* = 8.0 Hz, 1H), 1.853-1.696 (m, 2H), 1.015 (t, *J* = 7.5 Hz, 3H).

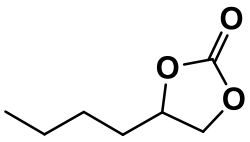

2c

4-butyl-1,3-dioxolan-2-one (2c): 87% yield; ^{1}H NMR (500 MHz, $CDCl_3$): δ = 4.697 (m, 1H), 4.522 (t, *J* = 8.0 Hz, 1H), 4.065 (t, *J* = 7.5 Hz, 1H), 1.845-1.772 (m, 1H), 1.717-1.648 (m, 1H), 1.493-1.319 (m, 4H), 0.922 (t, *J* = 7.0 Hz, 3H).

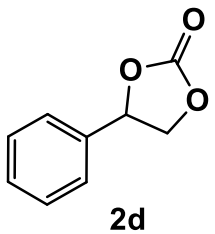

2d

4-phenyl-1,3-dioxolan-2-one (2d): 96% yield; ^{1}H NMR (500 MHz, $CDCl_3$): δ = 7.469-7.411 (m, 3H), 7.375-7.358 (m, 2H), 5.679 (t, *J* = 8.0 Hz, 1H), 4.804 (t, *J* = 8.5 Hz, 1H), 4.349 (t, *J* = 8.5 Hz, 1H).

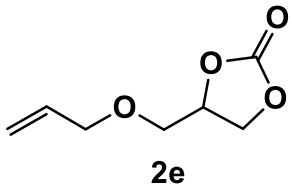

2e

4-[(Allyloxy)methyl]-1,3-dioxolan-2-one (2e): 99% yield; ^{1}H NMR (500 MHz, $CDCl_3$): *δ* = 5.898-5.820 (m, 1H), 5.275 (dd, J_1 = 17.5 Hz, J_2 = 1.0 Hz, 1H), 5.213 (d, *J* = 10.5 Hz, 1H), 4.839-4.795 (m, 1Hz), 4.495 (t, *J* = 8.5 Hz, 1H), 4.392 (dd, J_1 = 8.5 Hz, J_2 = 5.5 Hz, 1H), 4.047 (t, *J* = 5.0 Hz, 2H), 3.684 (dd, J_1 = 11.0 Hz, J_2 = 4.0 Hz, 1H), 3.608 (dd, J_1 = 11.0 Hz, J_2 = 4.0 Hz, 1H).

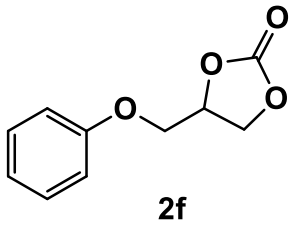

2f

4-phenyloxymethyl-1,3-dioxolan-2-one (2f): 99% yield; ^{1}H NMR (500 MHz, $CDCl_3$): *δ* = 7.312 (t, *J* = 8.0 Hz, 2H), 7.020 (t, *J* = 7.0 Hz, 1H), 6.914 (d, *J* = 8.5 Hz, 2H), 5.034 (m, 1H), 4.622 (t, *J* = 8.5 Hz, 1H), 4.548 (dd, J_1 = 9.0 Hz, J_2 = 6.0 Hz, 1H), 4.244 (dd, J_1 = 10.5 Hz, J_2 = 4 Hz, 1H), 4.154 (dd, J_1 = 10.5 Hz, J_2 =4.0 Hz, 1H).

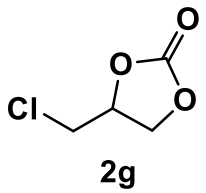

2g

4-chloromethyl-1, 3-dioxolan-2-one (2g): 98% yield; ^{1}H NMR (500 MHz, $CDCl_3$):*δ* = 4.994-4.948 (m, 1H), 4.588 (t, *J* = 8.5 Hz, 1H), 4.407 (dd, J_1 = 9 Hz, J_2 = 5.5 Hz, 1H), 3.785 (dd, J_1 = 12.0 Hz, J_2 = 5.5 Hz, 1H), 3.724 (dd, J_1 = 12 Hz, J_2 = 4.0 Hz, 1H).

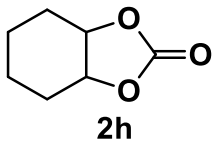

2h

4, 5- cyclohexyl-1, 3-dioxolan-2-one (2h): 67% yield; ^{1}H NMR (500 MHz, $CDCl_3$): δ = 4.696-4.656 (m, 2H), 1.891 (m, 4H), 1.653-1.583 (m, 2H), 1.447-1.378 (m, 2H).

1.18 Typical procedure for recycling binary BAAs/PGILs catalysts in coupling reaction of CO_2 with epoxides

Under an Argon atmosphere, SC (10.5 mmol) and binary catalyst *L*-Arg/[Me(EO)$_{16}$TMG-H][I] (0.105 mmol/0.105 mmol) were charged in a 60 mL stainless-steel autoclave equipped with a magnetic stirrer. The reaction mixture was heated to 110 °C, and then 1.5 MPa of CO_2 was introduced to autoclave. The reaction was carried out at 110 °C for 5 h, and the autoclave was cooled to room temperature in ice water. After CO_2 was slowly released, methyl *tert*-butyl ether was added to extract the resulting products. The upper organic phase was separated, and the catalyst phase was supplemented with fresh SC for the next catalytic cycle.

2 C1s XPS spectra of [Me(EO)$_{16}$TMG-H][Br], [TMG-H][Br], *L*-Arg/[Me(EO)$_{16}$TMG-H][Br] and *L*-Arg/[TMG-H][Br]

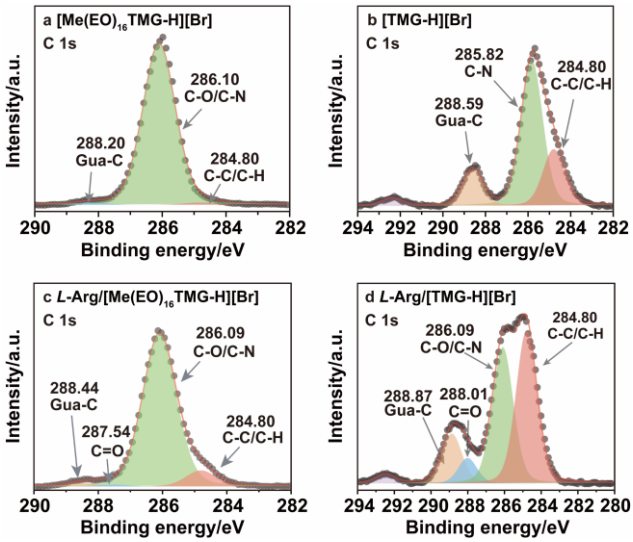

Figure S1. C 1s XPS spectra of (a) [Me(EO)$_{16}$TMG-H][Br], (b) [TMG-H][Br], (c) *L*-Arg/[Me(EO)$_{16}$TMG-H][Br] and (d) *L*-Arg/[TMG-H][Br].

3 Structure characterizations of binary *L*-Arg/[Me(EO)$_{16}$TMG-H][Br] catalyst

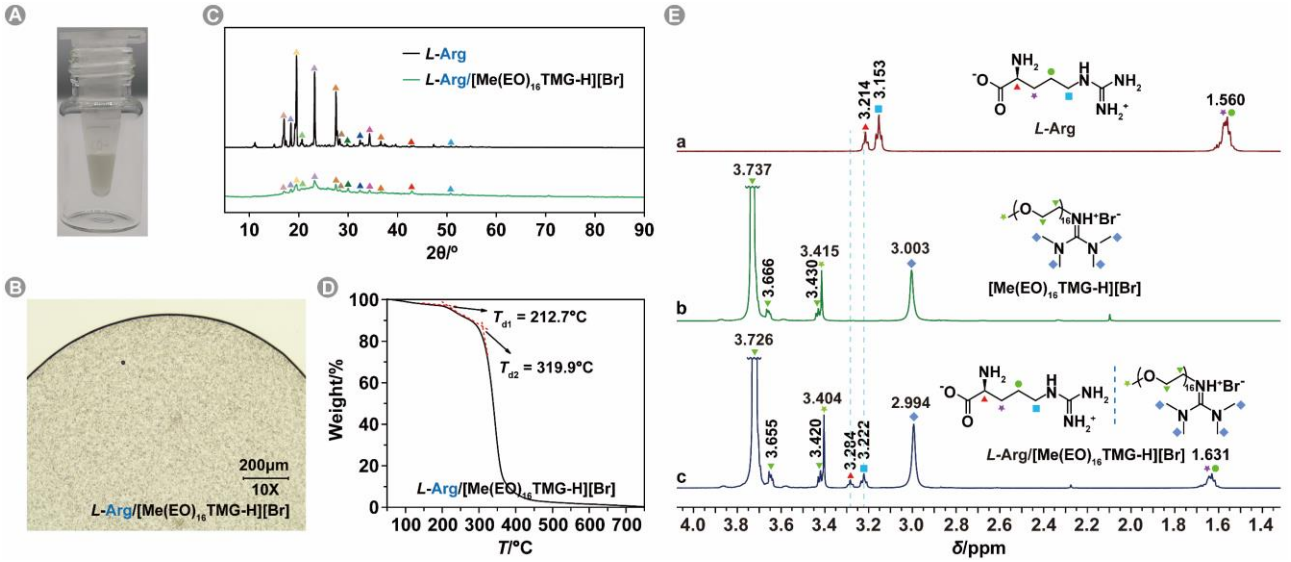

Figure S2. Structure characterizations of binary *L*-Arg/[Me(EO)$_{16}$TMG-H][Br] catalyst. (A) external photos, (B) optical microscopic images, (C) XRD patterns and (D) TG profiles of *L*-Arg/[Me(EO)$_{16}$TMG-H][Br]. (E) ^{1}H NMR spectra (500.0 MHz, D_2O) of (a) *L*-Arg, (b) [Me(EO)$_{16}$TMG-H][Br] and (c) *L*-Arg/[Me(EO)$_{16}$TMG-H][Br].

4 2D ROESY NMR spectrum of *L*-Arg + [Me(EO)$_{16}$TMG-H][Br]

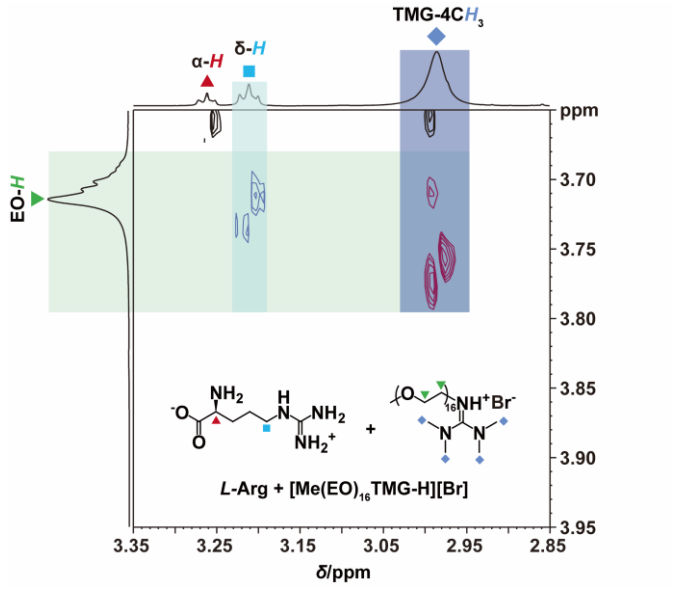

Figure S3. 2D ROESY NMR spectra (600.0 MHz, D_2O) of *L*-Arg + [Me(EO)$_{16}$TMG-H][Br] (298 K, 0.096 M/0.096 M). Arginine and [Me(EO)$_{16}$TMG-H][Br] were added separately into D_2O without prior physical doping.

5 The reaction kinetic study expressed as curves for TON *versus* time for the CO_2/SO coupling catalyzed by the binary catalysts *L*-Arg/[Me(EO)$_{16}$TMG-H][I] and *L*-Arg/[TMG-H][I]

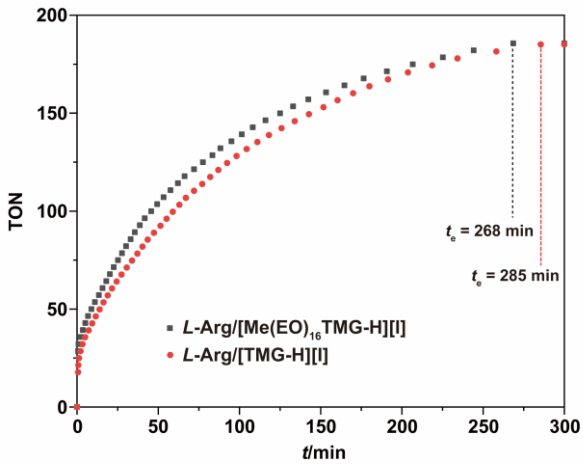

Figure S4. The reaction kinetic study expressed as curves for TON *versus* time for the CO_2/SO coupling catalyzed by the binary catalysts *L*-Arg/[Me(EO)$_{16}$TMG-H][I] and *L*-Arg/[TMG-H][I]. Reaction conditions: SO 10.5 mmol, 0.5 mol%/0.5 mol%, 1.5 MPa CO_2 at 110 °C, biphenyl (internal standard) 0.1 g; t_e: the end points of CO_2/SO coupling reactions.

6 The catalyst stability tested by recycle experiments and corresponding kinetic curves of TON *versus* time in the CO_2/SO coupling reaction using the binary *L*-Arg/[TMG-H][I] catalyst

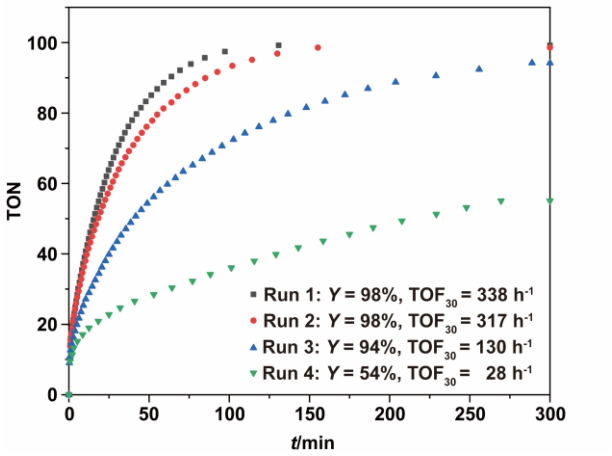

Figure S5. The catalyst stability tested by recycle experiments and corresponding kinetic curves of TON *versus* time in the CO_2/SO coupling reaction using the binary *L*-Arg/[TMG-H][I] catalyst. Reaction conditions: SO 10.5 mmol, 1.0 mol%/1.0 mol%, 1.5 MPa CO_2 at 110 °C, 5 h.

7 The catalyst stability characterized by ^{1}H NMR and FT-IR spectra of *L*-Arg/[Me(EO)$_{16}$TMG-H][I] catalyst in cycloaddition reaction of CO_2 and SO

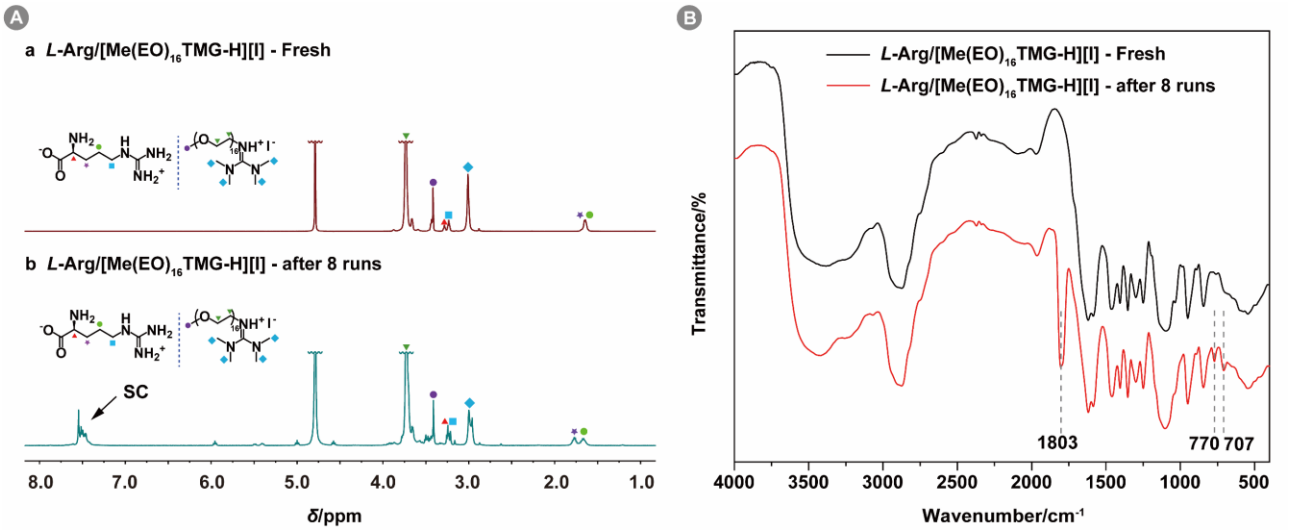

Figure S6. The catalyst stability characterized by (A) ^{1}H NMR and (B) FT-IR spectra of *L*-Arg/[Me(EO)$_{16}$TMG-H][I] catalyst in cycloaddition reaction of CO_2 and SO. Reaction conditions: SO 10.5 mmol, 1.0 mol%/1.0 mol%, 1.5 MPa CO_2 at 110 °C, 5 h.

8 Partial ^{1}H NMR spectra of [*L*-Arg-H][Br]/PO/PC and [Me(EO)$_{16}$TMG-H][Br]/PO/PC for recognizing the activation of PO by H-bonding

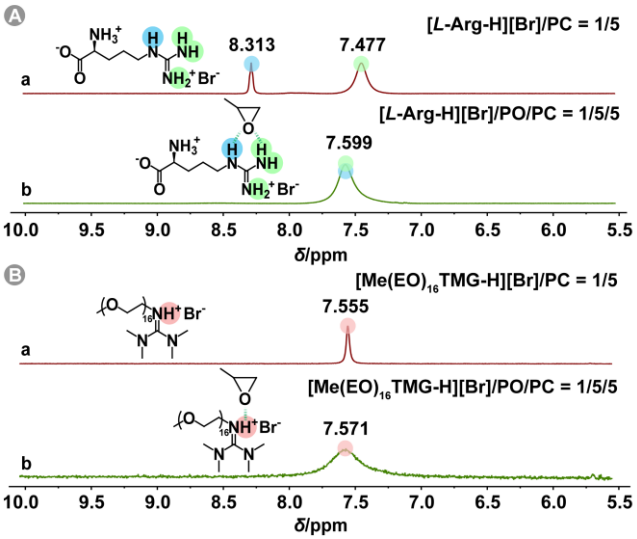

Figure S7. Partial ^{1}H NMR spectra (500 MHz, DMSO-D_6) of (A) [*L*-Arg-H][Br]/PO/PC (1:5:5, mol/mol/mol) and (B) [Me(EO)$_{16}$TMG-H][Br]/PO/PC (1:5:5, mol/mol/mol) for recognizing the activation of PO by H-bonding. Treatment conditions: the catalyst and solvent PC were mixed at 120 °C for 2 h (Ar atmosphere), cooled to R.T., and PO was added, for 5 h.

9 Effect of reaction temperature on reaction kinetics in the CO_2/SO coupling reaction: evolution of ln[SO] with time at four different temperatures for *L*-Arg/[Me(EO)$_{16}$TMG-H][Br], *L*-Arg/[TMG-H][Br] and [Me(EO)$_{16}$TMG-H][Br] catalysts

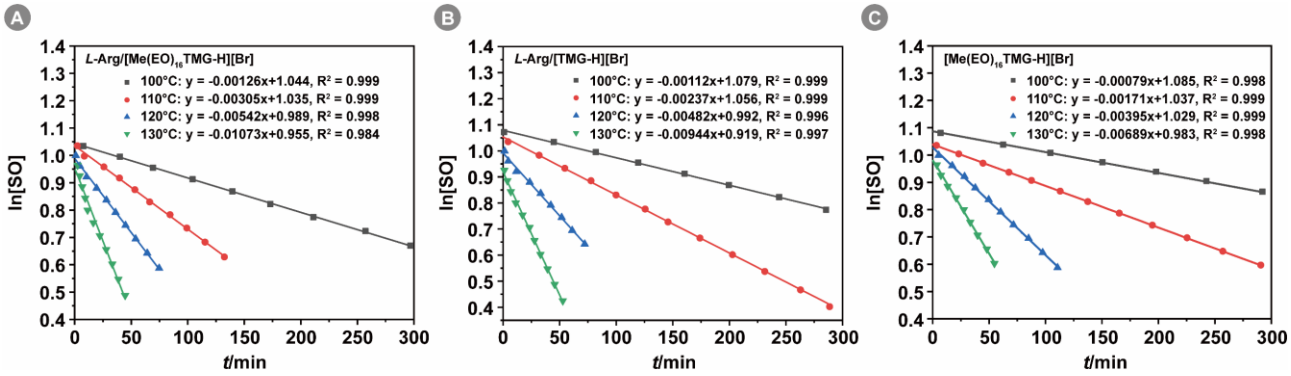

Figure S8. Effect of reaction temperature on reaction kinetics in the CO_2/SO coupling reaction: evolution of ln[SO] with time at four different temperatures for (A) *L*-Arg/[Me(EO)$_{16}$TMG-H][Br], (B) *L*-Arg/[TMG-H][Br] and (C) [Me(EO)$_{16}$TMG-H][Br] catalysts. Reaction conditions: SO 5.25 mmol, 0.6 mol%/0.6 mol% catalyst, 1.5 MPa CO_2, 1.2 mL PC as solvent.

10 NMR Spectra

10.1 ^{1}H NMR spectrum of [TMG-H][Br]

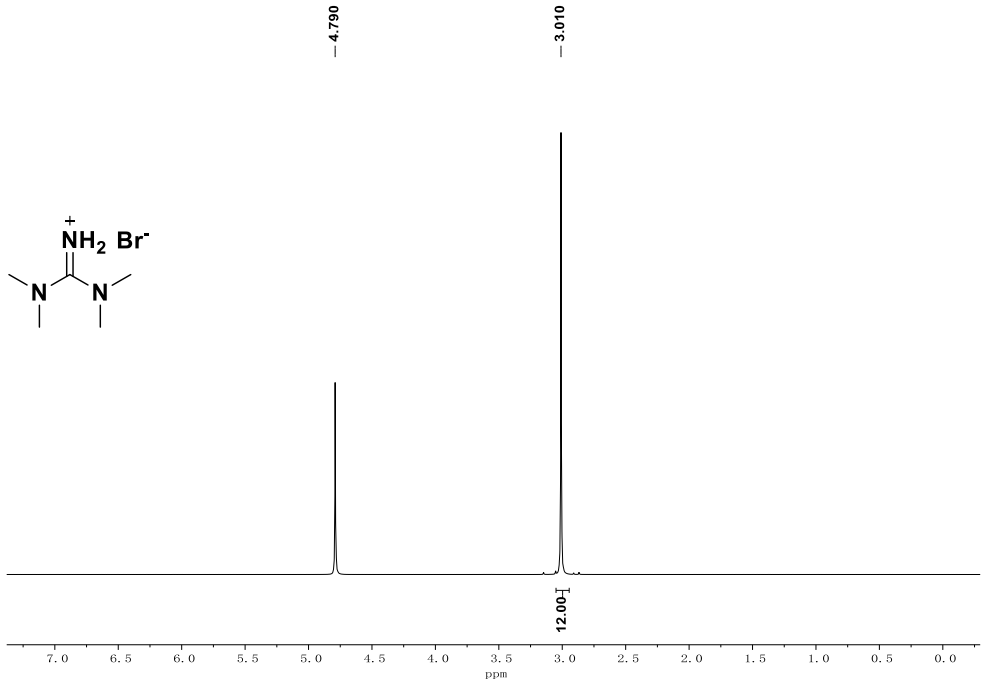

Figure S9. ^{1}H NMR spectrum of [TMG-H][Br] (500 MHz, D_2O)

10.2 ^{1}H NMR spectrum of [TMG-H][I]

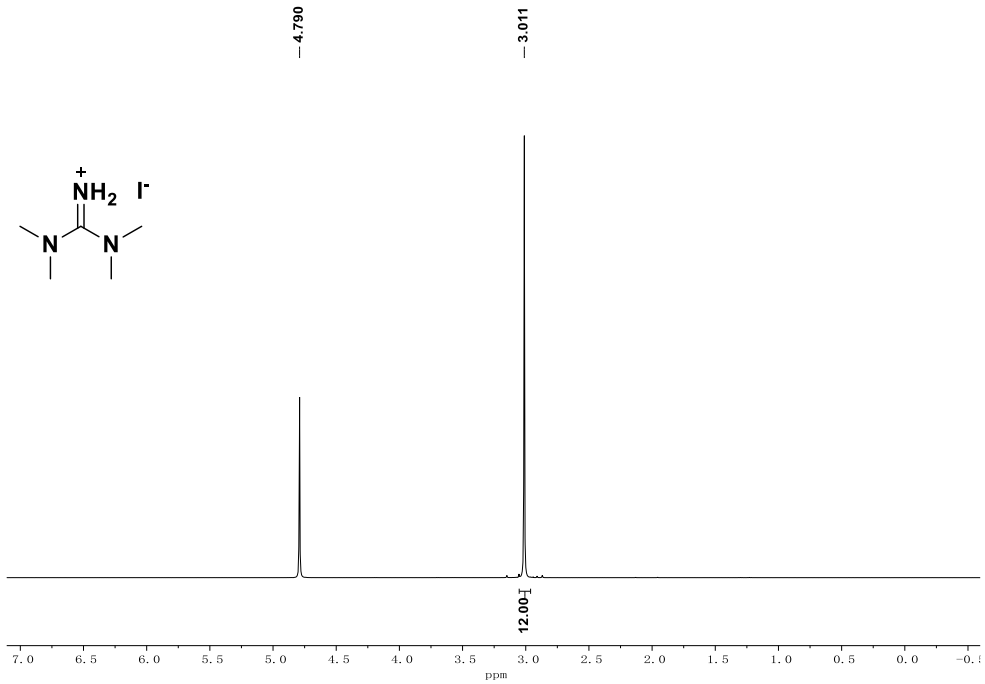

Figure S10. ^{1}H NMR spectrum of [TMG-H][I] (500 MHz, D_2O)

10.3 ^{1}H NMR spectrum of [MTBD-H][Br]

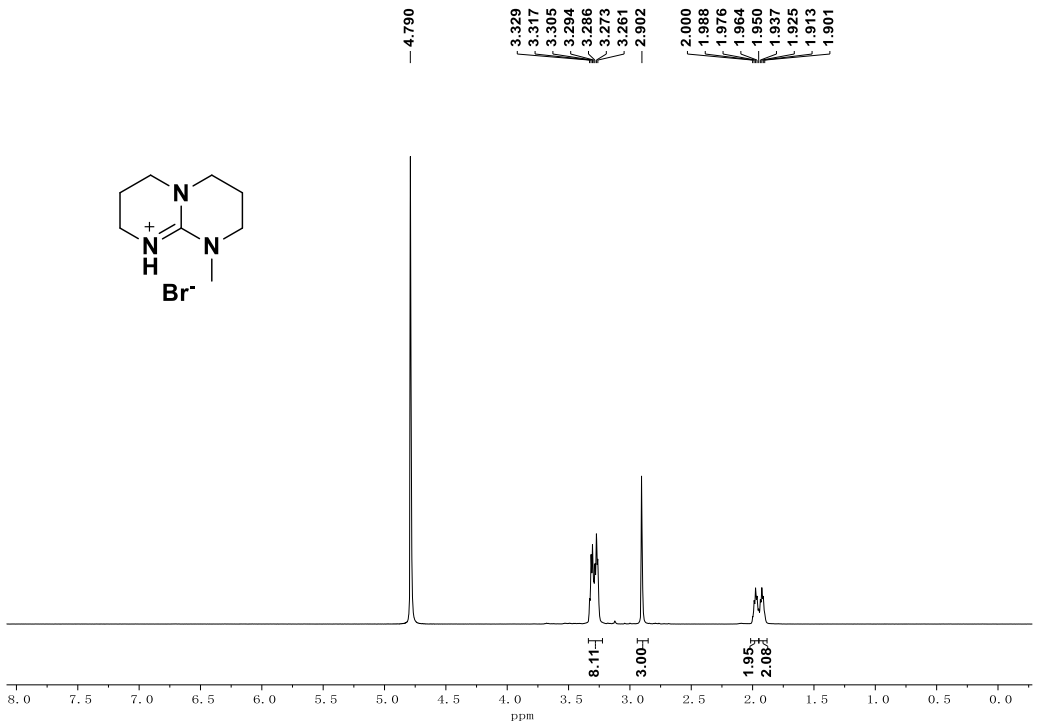

Figure S11. ^{1}H NMR spectrum of [MTBD-H][Br] (500 MHz, D_2O)

10.4 ^{1}H NMR spectrum of [Me(EO)$_4$TMG-H][Br]

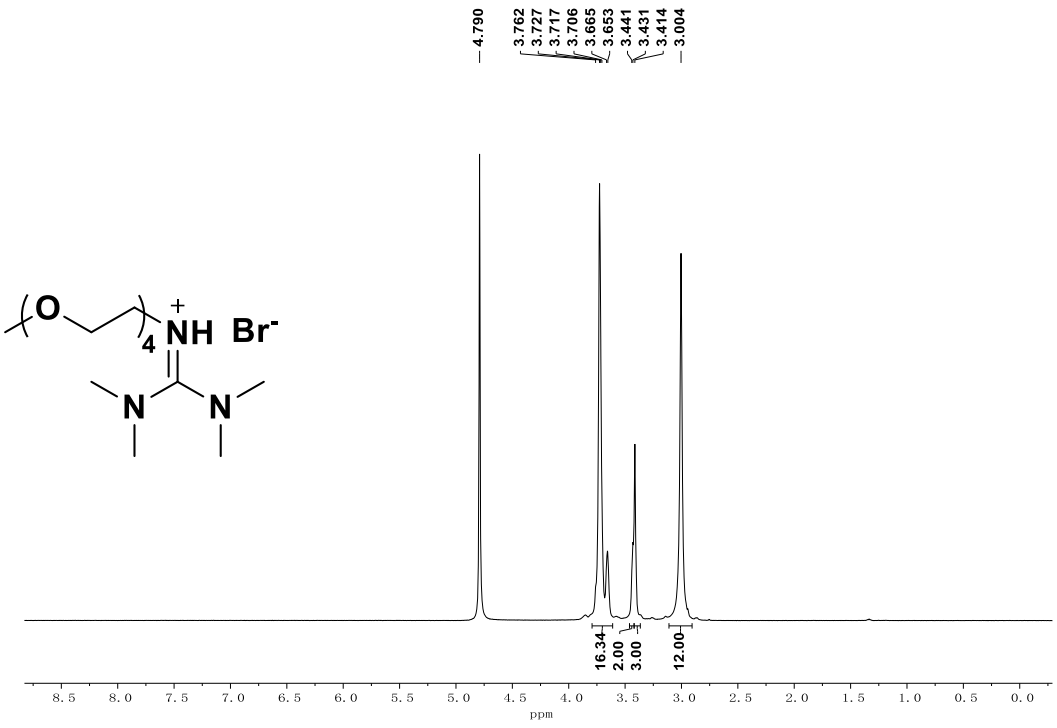

Figure S12. ^{1}H NMR spectrum of [Me(EO)$_4$TMG-H][Br] (500 MHz, D_2O)

10.5 ^{13}C NMR spectrum of [Me(EO)$_4$TMG-H][Br]

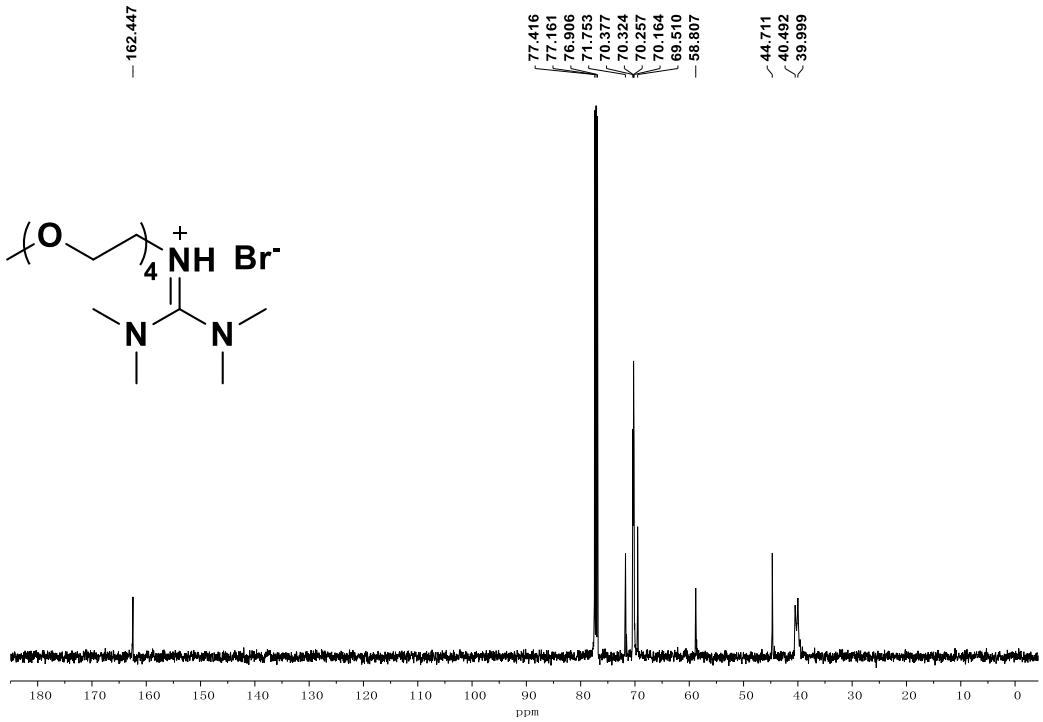

Figure S13. ^{13}C NMR spectrum of [Me(EO)$_4$TMG-H][Br] (126 MHz, $CDCl_3$)

10.6 ^{1}H NMR spectrum of [Me(EO)$_{16}$TMG-H][Br]

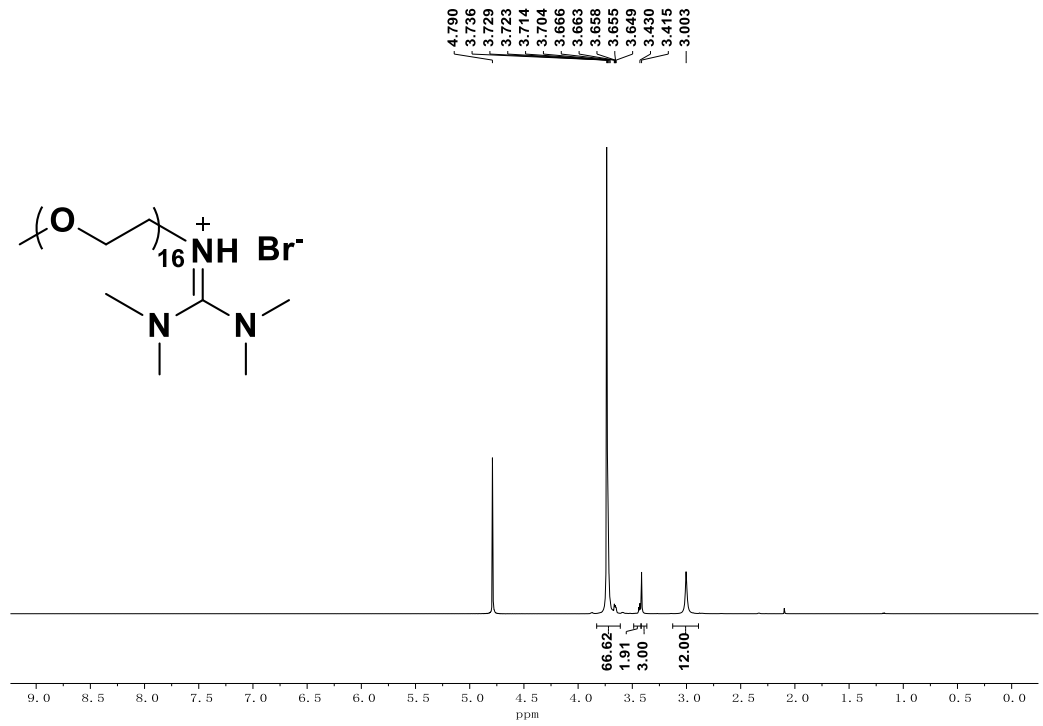

Figure S14. ^{1}H NMR spectrum of [Me(EO)$_{16}$TMG-H][Br] (500 MHz, D_2O)

10.7 ^{13}C NMR spectrum of [Me(EO)$_{16}$TMG-H][Br]

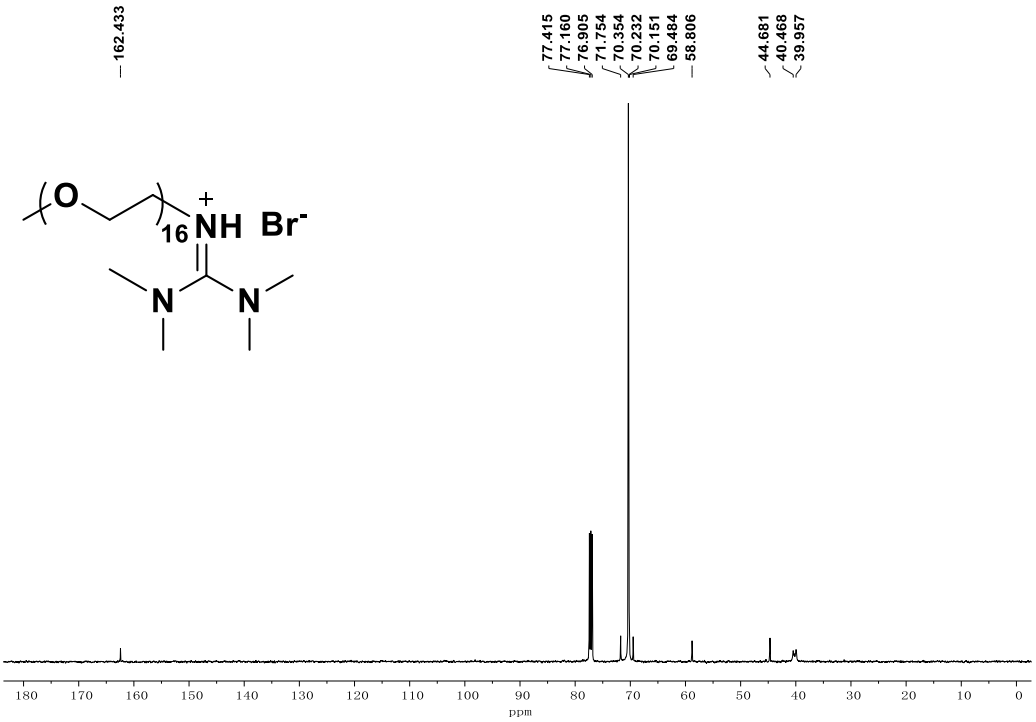

Figure S15. ^{13}C NMR spectrum of [Me(EO)$_{16}$TMG-H][Br] (126 MHz, $CDCl_3$)

10.8 ^{1}H NMR spectrum of [Me(EO)$_{16}$TMG-H][I]

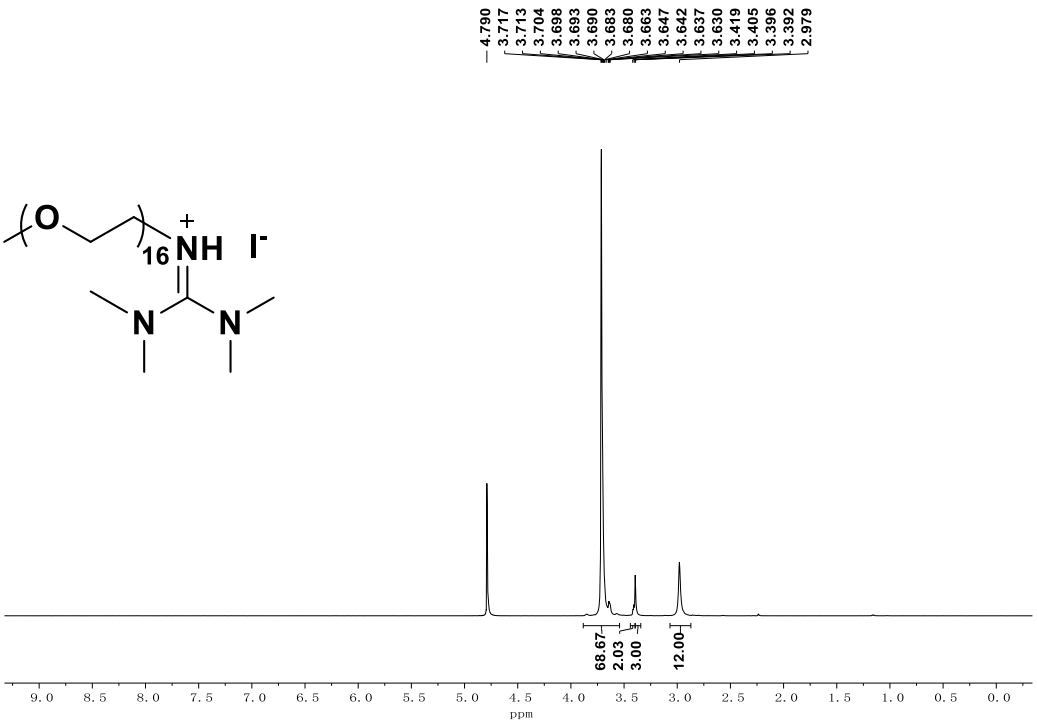

Figure S16. ^{1}H NMR spectrum of [Me(EO)$_{16}$TMG-H][I] (500 MHz, D_2O)

10.9 ^{13}C NMR spectrum of [Me(EO)$_{16}$TMG-H][I]

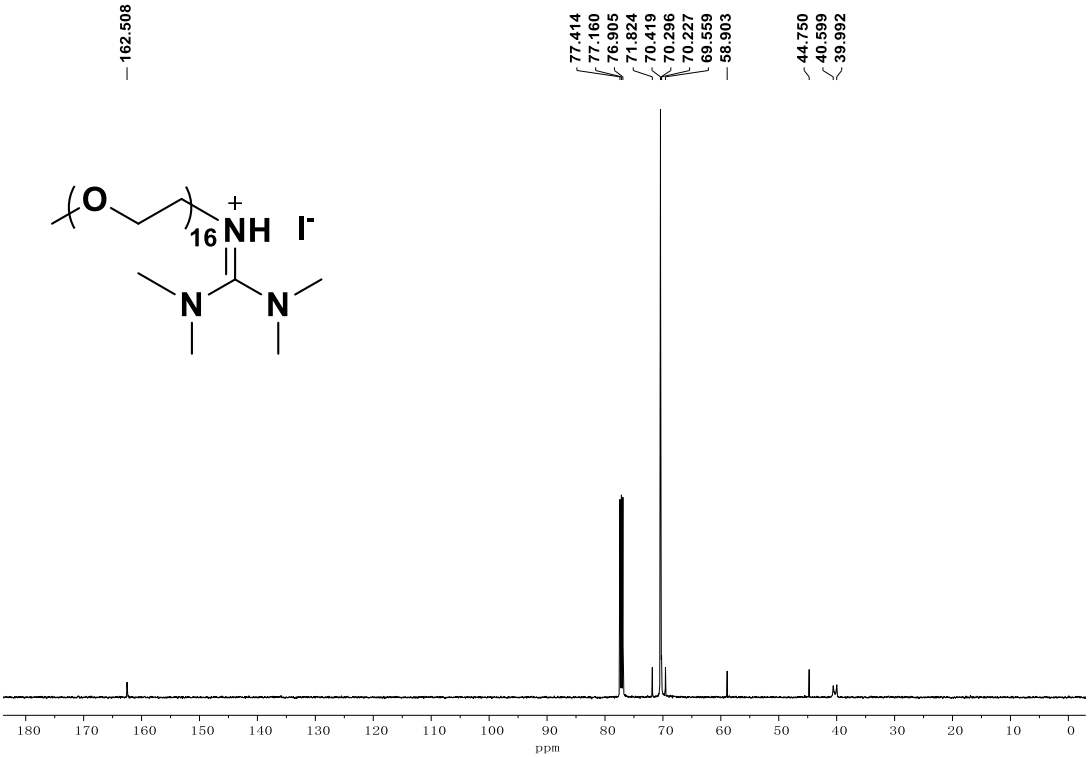

Figure S17. ^{13}C NMR spectrum of [Me(EO)$_{16}$TMG-H][I] (126 MHz, $CDCl_3$)

10.10 ^{1}H NMR spectrum of **2a**

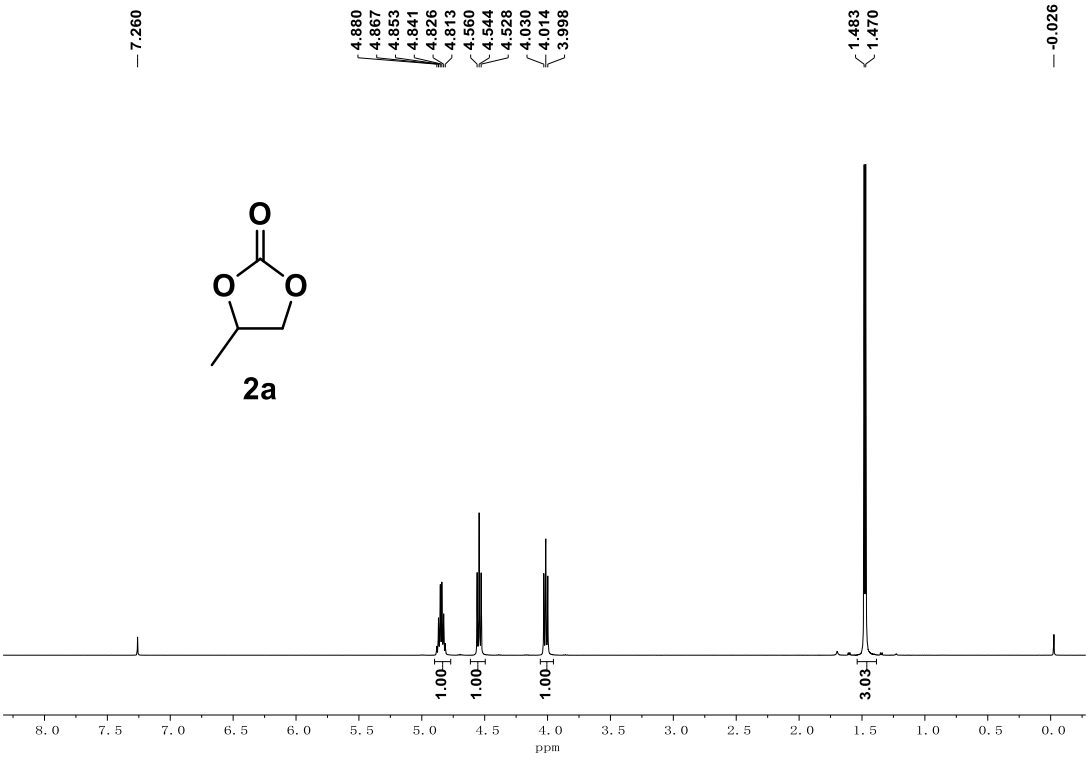

Figure S18. ^{1}H NMR spectrum of **2a** (500 MHz, $CDCl_3$)

10.11 ^{1}H NMR spectrum of **2b**

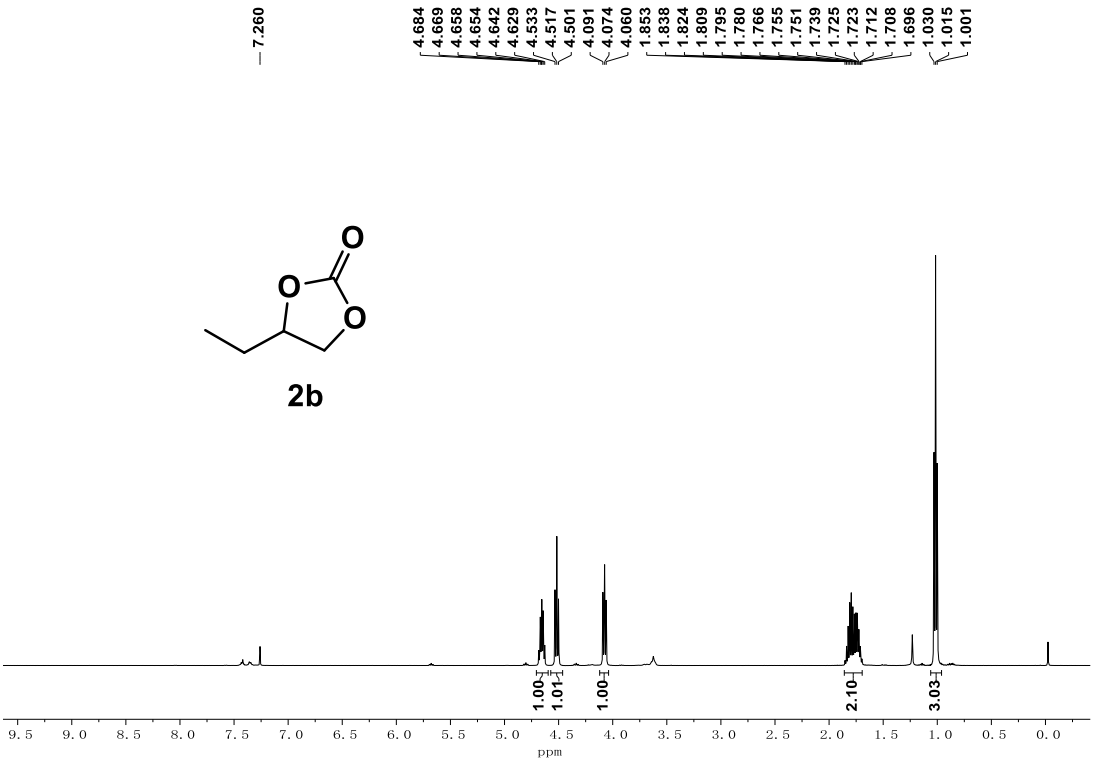

Figure S19. ^{1}H NMR spectrum of **2b** (500 MHz, $CDCl_3$)

10.12 ^{1}H NMR spectrum of **2c**

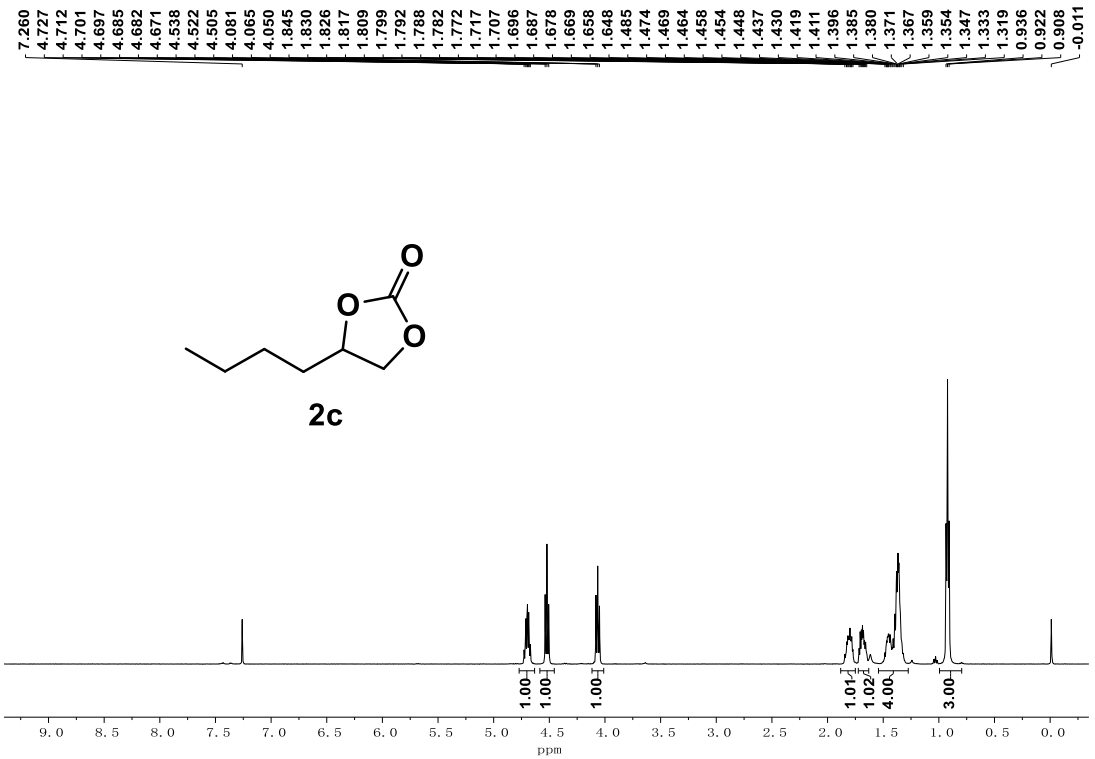

Figure S20. ^{1}H NMR spectrum of **2c** (500 MHz, $CDCl_3$)

10.13 ^{1}H NMR spectrum of **2d**

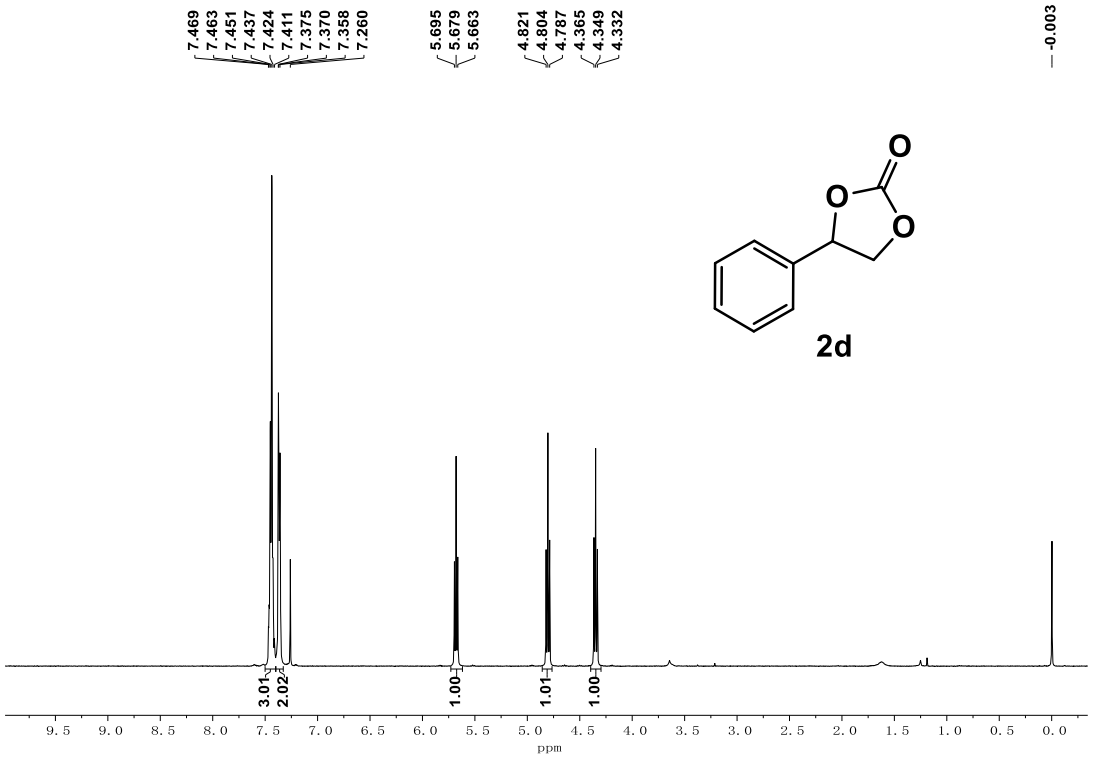

Figure S21. ^{1}H NMR spectrum of **2d** (500 MHz, $CDCl_3$)

10.14 ^{1}H NMR spectrum of **2e**

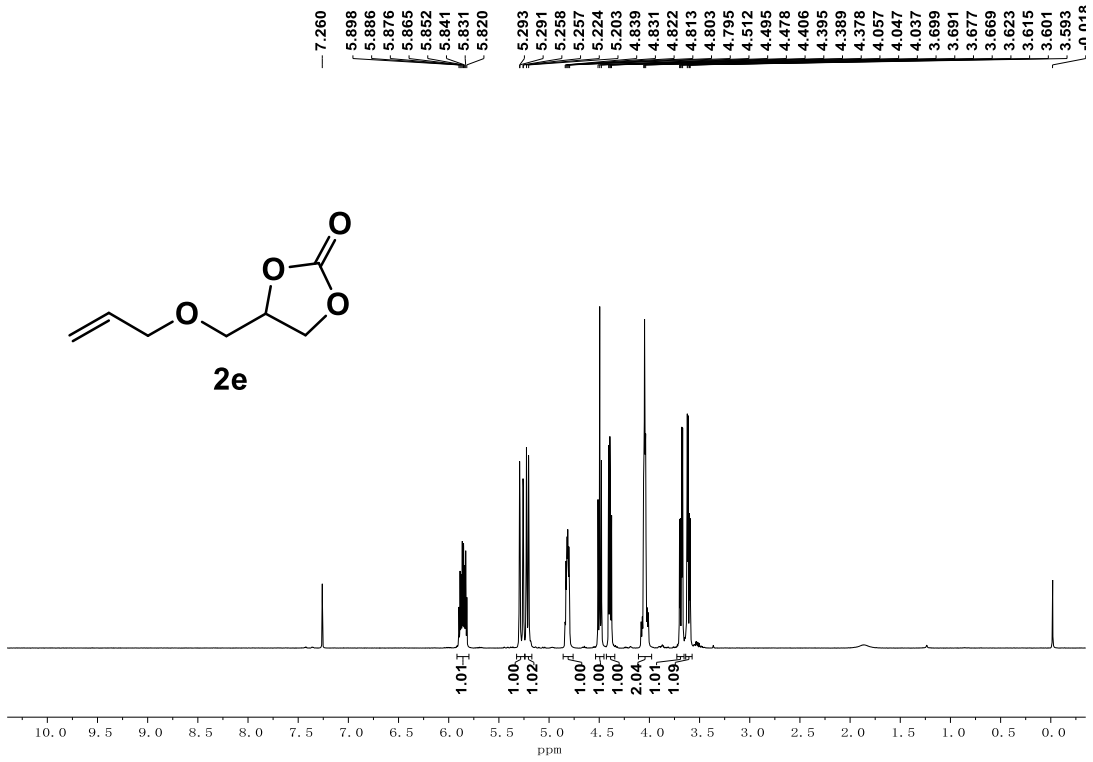

Figure S22. ^{1}H NMR spectrum of **2e** (500 MHz, $CDCl_3$)

10.15 ^{1}H NMR spectrum of **2f**

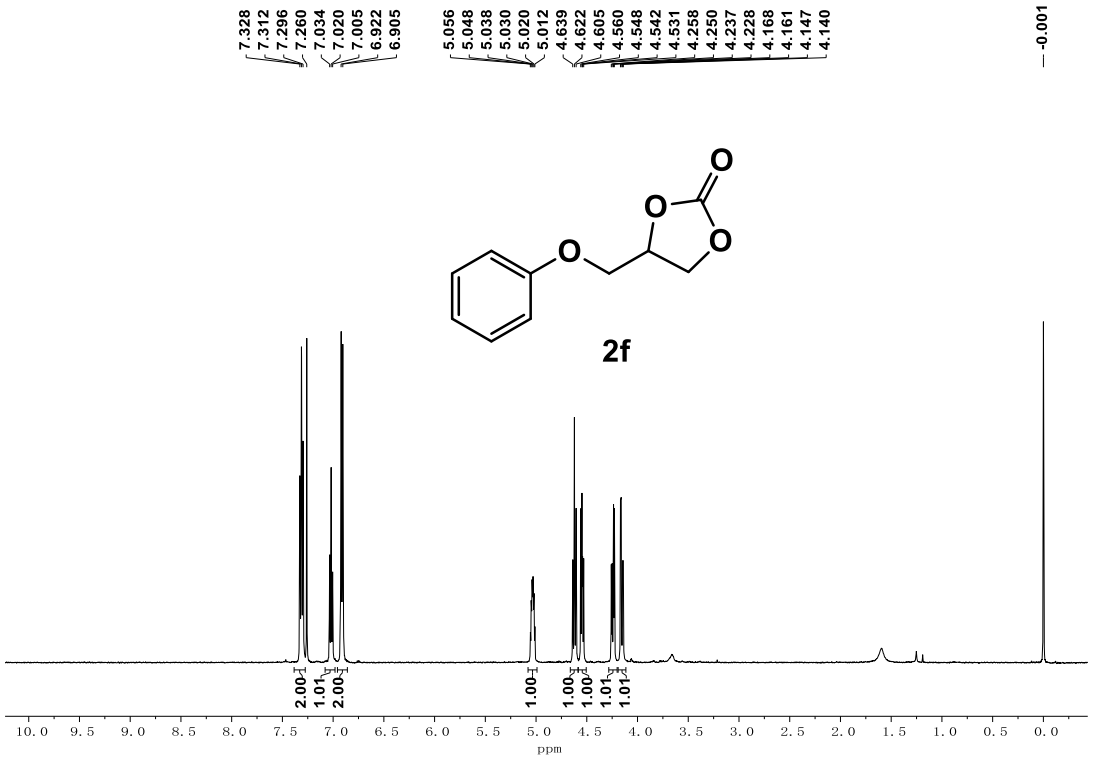

Figure S23. ^{1}H NMR spectrum of **2f** (500 MHz, $CDCl_3$)

10.16 ^{1}H NMR spectrum of **2g**

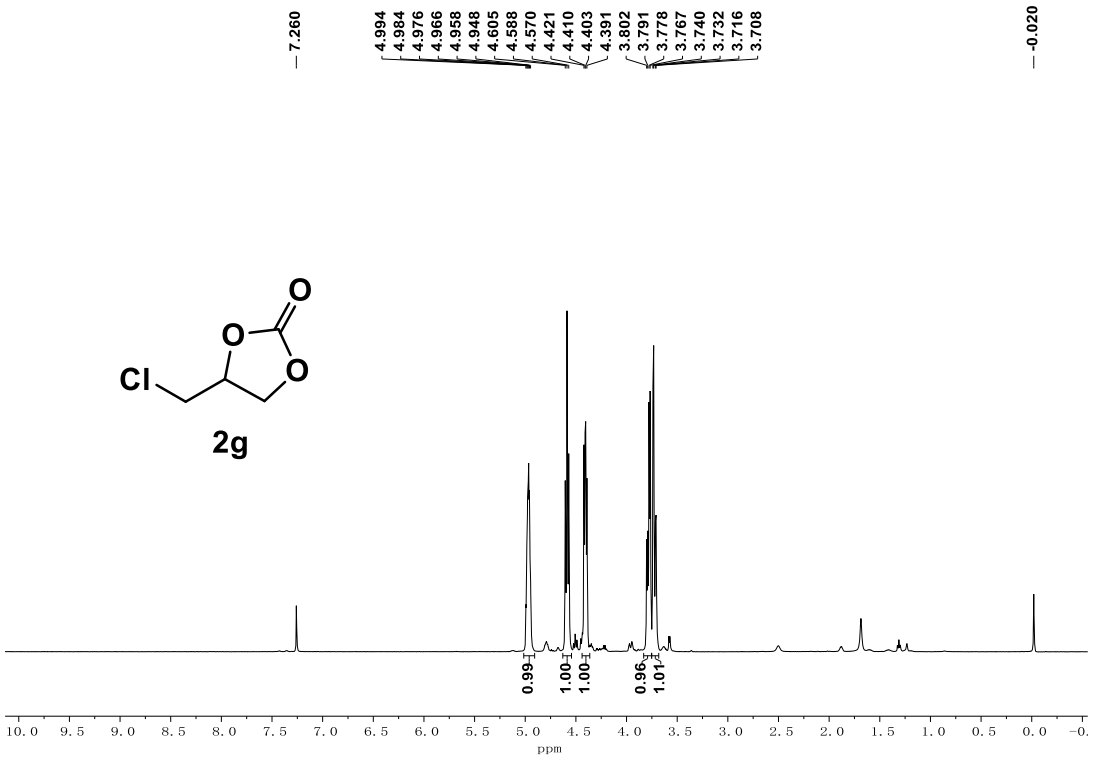

Figure S24. ^{1}H NMR spectrum of **2g** (500 MHz, $CDCl_3$)

10.17 ^{1}H NMR spectrum of **2h**

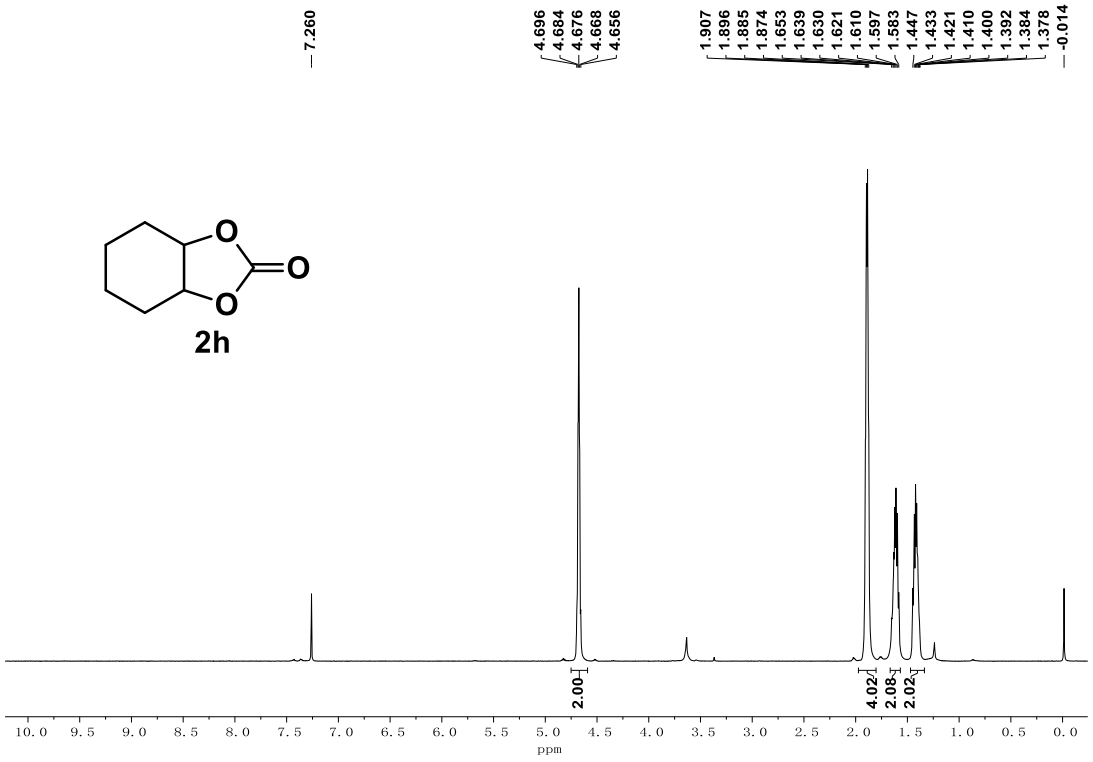

Figure S25. ^{1}H NMR spectrum of **2h** (500 MHz, $CDCl_3$)

11 MS Spectra

11.1 Mass spectrum (ESI positive) of [Me(EO)$_4$TMG-H][Br]

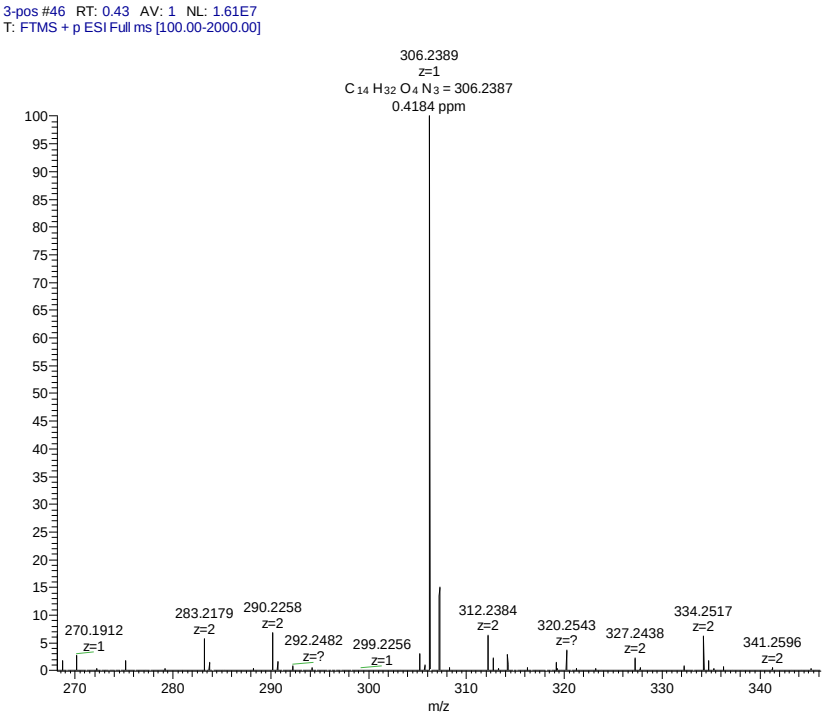

Figure S26. Mass spectrum (ESI positive) of [Me(EO)$_4$TMG-H][Br]

11.2 Mass spectrum (ESI negative) of [Me(EO)$_4$TMG-H][Br]

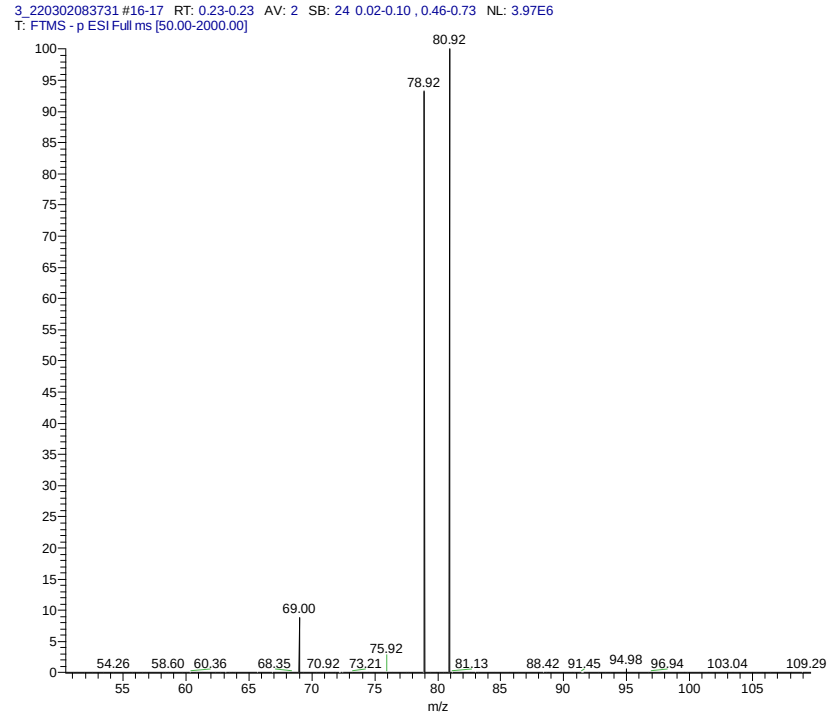

Figure S27. Mass spectrum (ESI negative) of [Me(EO)$_4$TMG-H][Br]

11.3 Mass spectrum (ESI positive) of [Me(EO)$_{16}$TMG-H][Br]

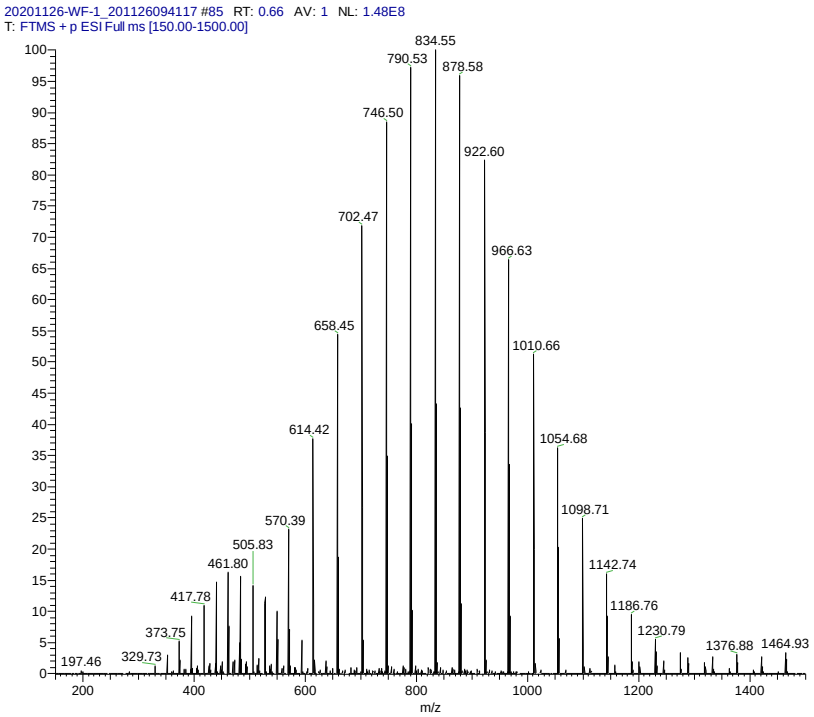

Figure S28. Mass spectrum (ESI positive) of [Me(EO)$_{16}$TMG-H][Br]

11.4 Mass spectrum (ESI negative) of [Me(EO)$_{16}$TMG-H][Br]

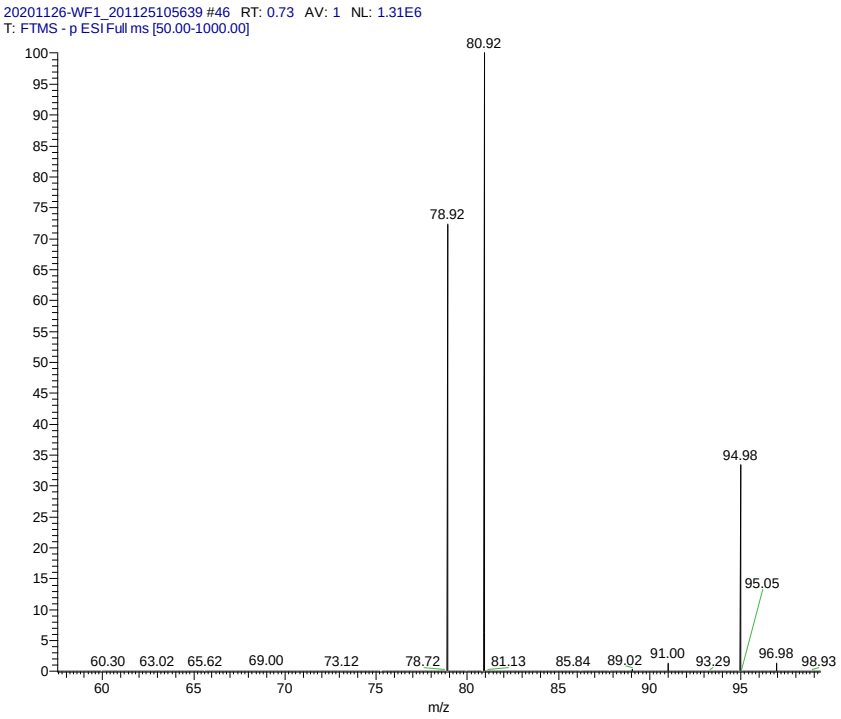

Figure S29. Mass spectrum (ESI negative) of [Me(EO)$_{16}$TMG-H][Br]

11.5 Mass spectrum (ESI positive) of [Me(EO)$_{16}$TMG-H][I]

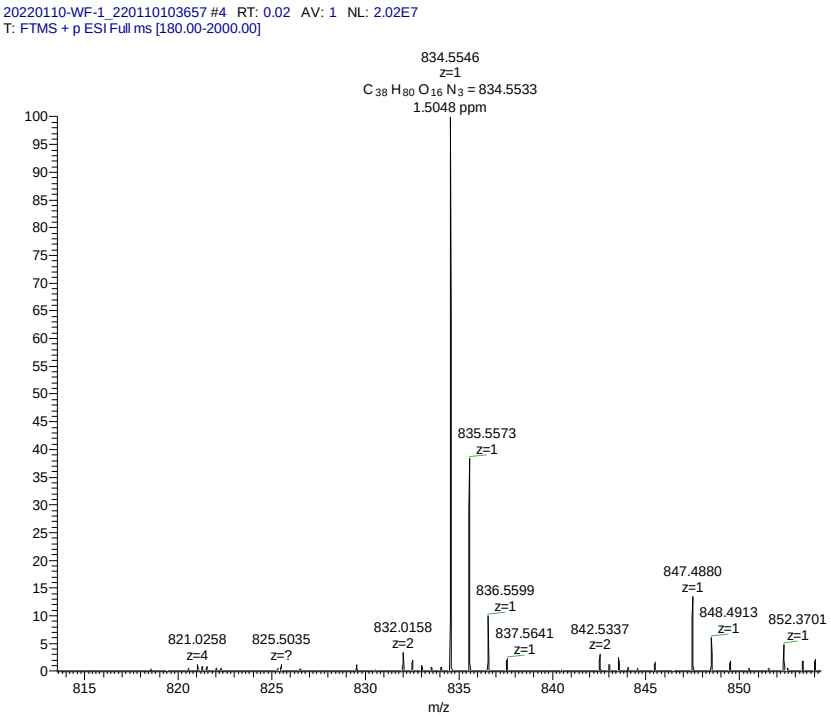

Figure S30. Mass spectrum (ESI positive) of [Me(EO)$_{16}$TMG-H][I]

11.6 Mass spectrum (ESI negative) of [Me(EO)$_{16}$TMG-H][I]

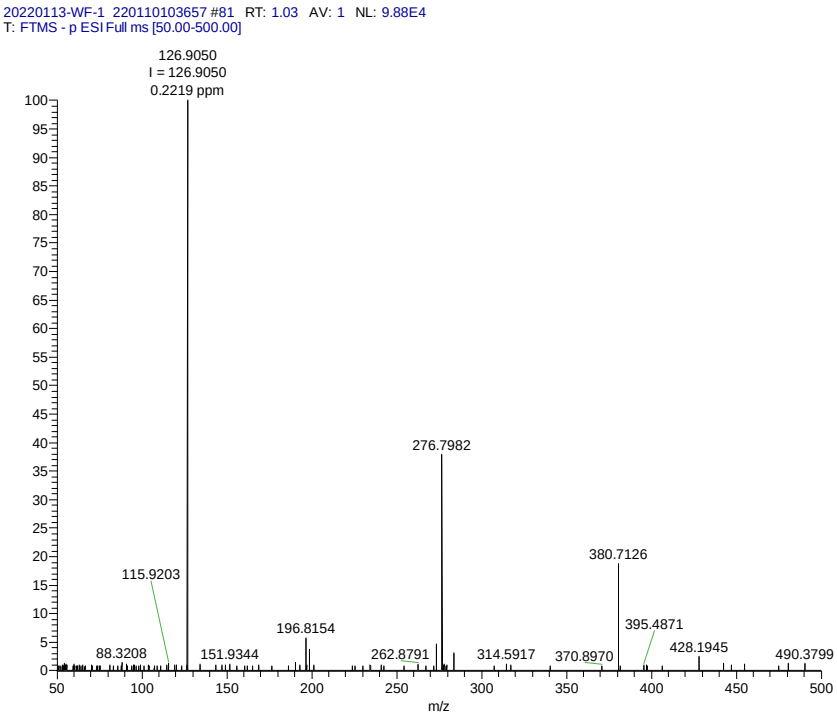

Figure S31. Mass spectrum (ESI negative) of [Me(EO)$_{16}$TMG-H][I]

References

1 W. L. F. Armarego and C. L. L. Chai, *Purification of Laboratory Chemicals*, Elsevier/Butterworth-Heinemann, Burlington, MA, USA, 5th edn, 2003.

2 X. Jin, D. Yang, X. Xu and Z. Yang, *Chem. Commun.* 2012, **48**, 9017–9019.